ceramics

MDPI

Non-Oxide Ceramics for Bone Implant Application: State-of-the-Art Overview with an Emphasis on the Acetabular Cup of Hip Joint Prosthesis

Consiglio M. Paione and Francesco Baino *

Institute of Materials Physics and Engineering, Department of Applied Science and Technology, Politecnico di Torino, 10129 Turin, Italy
* Correspondence: francesco.baino@polito.it

Abstract: A rapidly developing area of ceramic science and technology involves research on the interaction between implanted biomaterials and the human body. Over the past half century, the use of bioceramics has revolutionized the surgical treatment of various diseases that primarily affect bone, thus contributing to significantly improving the quality of life of rehabilitated patients. Calcium phosphates, bioactive glasses and glass-ceramics are mostly used in tissue engineering applications where bone regeneration is the major goal, while stronger but almost inert biocompatible ceramics such as alumina and alumina/zirconia composites are preferable in joint prostheses. Over the last few years, non-oxide ceramics—primarily silicon nitride, silicon carbide and diamond-like coatings—have been proposed as new options in orthopaedics in order to overcome some tribological and biomechanical limitations of existing commercial products, yielding very promising results. This review is specifically addressed to these relatively less popular, non-oxide biomaterials for bone applications, highlighting their potential advantages and critical aspects deserving further research in the future. Special focus is also given to the use of non-oxide ceramics in the manufacturing of the acetabular cup, which is the most critical component of hip joint prostheses.

Keywords: bioceramics; hip joint prosthesis; silicon carbide; silicon nitride; DLC

1. Introduction

Although the outcomes of bone implants have been improved dramatically over the last decades, failure is still highly present in the literature, especially in dental, hip or knee replacement implants. Failure can be determined by a number of patient-, material- or surgery-related issues, such as immune system rejection, inflammation, allergy, accidents, surgical operation problems and complications, chemical corrosion or mechanical failure. In over 60,000 publications about prostheses on the ISI Web of Knowledge database dating from 1900 to 2019, about 9500, or approximately 15%, report failure of some kind, 26% of which indicate failure caused by the material, which is about 4% of the total number of publications [1]. Of course, these aggregate results over such a long period of time might misrepresent the improvement seen in more recent times, and they do not account for how different types of prostheses are more or less prone to failure. Nevertheless, such data are still representative of the impact that material choice alone can have on the overall success of prosthetics. Half of the studies are focused on hard tissues and joints, which are structural components of the human body. Despite research efforts, the incidence of failure caused by materials in hip prostheses-related publications is 5%, and jaw implants show a much higher failure rate (13%), as they are geometrically complex and subject to cyclic loading and varying liquid environments (Figure 1). Interestingly, knee implants are half as likely to fail compared to their hip counterpart, while also being slightly more researched (about 1600 versus 1300 publications). On the other hand, revision surgery data in more recent studies show a 10% probability of revision surgery 15 years after THR. The revision

rates increase to 30% at 20 years and further up to 40% at 35 years after initial surgery, strongly suggesting the need for improvement [2]. While it has to be pointed out that aggregate revision rates are dependent on many factors that are not only material-related, long-term revisions are more often caused by aseptic loosening, metallosis, bearing wear and other factors that are directly or indirectly connected with material choice [3]. SiC, Si_3N_4 and diamond-like carbon have been used in plenty of applications, yet there is still debate over what they can bring to bone implants in general and what they can do for the acetabular cup in hip prostheses in particular. Bone implant applications of these materials in the form of non-porous/porous products, as well as coatings and in bulk form, will be discussed in the present review, with a focus on mechanical properties, tribology and biocompatibility while also exploring some innovative manufacturing processes.
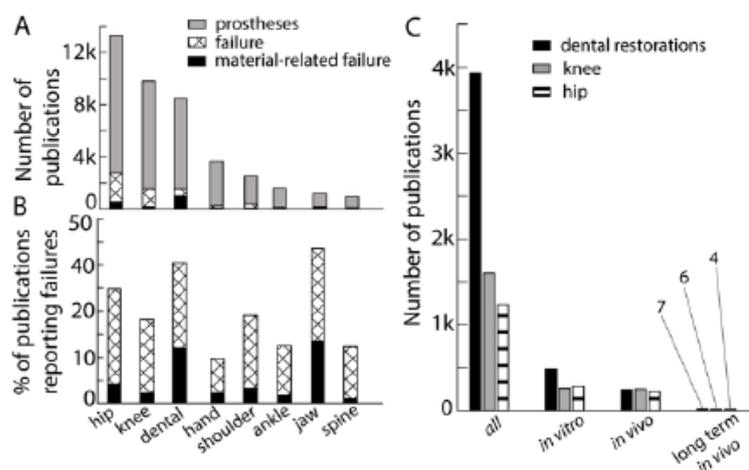

Figure 1. (**A**) Number of publications by bone implant type and absolute number that is related to failure; (**B**) percentage of failure-related publications by implant type; (**C**) research volume of the four most researched implants, by research type [1].

2. Evolution of Bone Implant Materials and Ceramics for Osseous Applications

A brief description of the evolution of materials used in bone prostheses might be useful to understand where research is currently headed and why ceramic materials still look promising. Although challenges in the field remain many, the progress achieved so far should not be overlooked. While the whole topic of bone implants can be traced back as early as 2000 B.C., only in the 20th century did an articulate approach to the matter emerge, with a focus on biocompatiblity and corrosion resistance, in addition to mechanical properties. In the 1900s, vanadium steel was invented for use in bone implants [4]; however, vanadium steel alone did not prove to be sufficient in withstanding the corrosion brought upon it by body fluids. In 1926, 316 AISI-SAE steel (18Cr-8Ni in ISO nomenclature) was first implemented for bone implant applications, proving superior to vanadium steel in terms of both strength and resistance to corrosion in vivo [5]. Later, in the 1950s, 316L stainless steel was introduced, the "L" standing for low carbon content (0.03 wt% compared to 0.08 wt% in standard 316 steel). The lower carbon content resulted in improved weldability and reduced corrosion sensitization, the major cause of intergranular corrosion. In the 1940s, titanium and its alloys were introduced into orthopaedic practice because of its good chemical behaviour in contact with body fluids, as experience from aircraft applications in those years showed remarkable seawater corrosion resistance. In vivo experiments confirmed the outstanding corrosion resistance, stimulating more research and leading to titanium being one of the most used biomaterials in bone prostheses. However, even with titanium, metallic ions release might occur to some extent over time. During the 1950s, properties of ultra high molecular weight polyethylene (UHMWPE) inspired biomedical applications of polymers due to its biocompatibility, lubrication, impact and abrasion resistance, making it a great artificial substitute for cartilage [6]. In the 1960s, the first total hip replacement (THR) operation was carried out by British orthopaedic surgeon Sir John Charnley, who

removed the femoral head and replaced it using a stainless-steel ball and a high-density PE (HDPE) socket inserted in the patient's acetabulum [7]. This proved revolutionary in the treatment of patients with arthritis, improving the quality of life of millions of people over the years. Even so, considering the permanent nature of these implants, polymers as a bearing surface raised some concerns because wear-derived PE particles tend to accumulate in the body and may result in the so-called "particle disease" or other situations where extra surgery is needed [8]. Also in the 1960s, another breakthrough in materials for structural bone implants took place with the advent of alumina and zirconia. They show great strength, hardness, resistance to corrosion and abrasion and, most importantly, high biocompatibility and chemical inertness (as shown in Table 1), thus being chemically stable in an oxidative environment such as the human body [9]. As a result, the use of oxide-based crystalline materials as bearing surfaces promises less contact surface wear, and hence less wear particles, and more biocompatibility. Nonetheless, like all ceramic materials, alumina is a brittle material exhibiting catastrophic failure, and experience in the field has raised concerns about that eventuality [10]. However, the properties of ceramic materials were simply too desirable to give up development on such implants. Adding zirconia into alumina, effectively creating a composite with increased fracture toughness and slower crack propagation, addressed the issue, but only to a limited extent. In recent times, however, other ceramic materials came to light, namely non-oxide ceramics, offering improved fracture toughness and strength (Table 2). Silicon nitride, silicon carbide and diamond-like carbon have been researched extensively in biomedical applications in the last few decades, with very promising results. Looking at the goals of ceramic implants for bone-contact applications, they are mainly addressed to (i) load-bearing structural functions, such as joint prostheses, and (ii) bone regeneration (filling and repair small orthopaedic/dental defects). The materials reviewed in this article typically belong to the former class and are usually fabricated as ideally pore-free products to ensure high mechanical properties (Table 2). The second class mainly encompasses oxide-based ceramics, both crystalline (e.g., hydroxyapatite) and amorphous (bioactive glasses), provided with inherent bone-bonding and osteo-stimulatory properties (see also Table 1). Such bioactive ceramics may be used in combination with other stronger materials, e.g., in the form of coatings on metallic implants [11] or as self-standing porous templates (scaffolds) allowing tissue regeneration in 3D [12]. Over the years, scientists have established a set of basic requirements that a scaffold for bone tissue engineering should ideally have, including total porosity above 50 vol.%, open-pore architecture, most macropores within 100–500 μm, high interconnectivity of pores, mechanical properties comparable to those of cancellous bone, degradation rate in the body matching the kinetics of bone ingrowth and relatively easy machineability [13]. Of course, a certain overlap may exist between the classes (i) and (ii) mentioned above; thus, some non-bioactive ceramics are produced in the form of strong, porous scaffolds allowing passive bone ingrowth.

Table 1. Major properties of oxide-based bioceramics (non-porous bulk) for medical applications (data from [14,15]).

Materials	Elastic Modulus [GPa]	Tensile Strength [MPa]	Compressive Strength [MPa]	Fracture Toughness [MPa $\cdot$ m$^{\frac{1}{2}}$]	Biological Behaviour
Alumina	400–450	250–300	2000–3000	4–5	inert
Zirconia	210	700	2000	8	inert
Hydroxyapatite	100	40	400	1	bioactive (osteoconductive)
45S5 Bioglass	35	45	500	0.5–1	bioactive (osteoinductive)

Table 2. Properties of silicon nitride and silicon carbide compared to other materials used in biomedical structural applications and cortical bone (data from [15,16]).

Materials	Density [kg/m^3]	Elastic Modulus [GPa]	Tensile Strength [MPa]	Compressive Strength [MPa]	Flexural Strength [MPa]	Fracture Toughness [MPa · m$^{\frac{1}{2}}$]
Si$_3$N$_4$	3150–3260	300–320	350–400	2500–3000	800–1100	8–11
SiC	3050	420	-	3900	280–428	4.6
Al$_2$O$_3$	3986	400–450	250–300	2000–3000	300–500	4–5
ZTA	4370	350	-	4300	1000	5.7
CoCr	8500	210–250	-	600–1800	-	50–100
PEEK	1290	4.2	100–110	130–140	160–180	-
Ti-alloy	4430	105–115	920–980	950–990	-	75
Bone	1900	8–12	50–130	130–190	-	1.7–5

3. Design and Challenges Associated with the Acetabular Cup

Over 1 million hip and knee replacement surgeries are carried out every year in the United States alone, and more than 7 million people are living with these implants. OECD (Organization for Economic Cooperation and Development) countries showed an increase of 22% in hip replacement rates between 2009 and 2019 [17]. Total hip replacement (THR) is used to treat patients with severe arthritis, which more frequently strikes the elderly. The ageing population in developed countries is going to increase demand even further, challenging the industry on both the availability and reliability of implants. However, younger people also undergo THR, creating a need for long-lasting implants, while at the same time, younger people tend to be more physically active, making the design objectives more ambitious. Although hip prostheses are widely researched implants, their design and material choice is still challenging, as emphasized, for example, in a critical review by Pezzotti and Yamamoto [18]. As previously discussed, various ceramic and metallic biomaterials are used today for THR, with the former typically offering the best biocompatibility and anti-wear properties and the latter providing higher fracture toughness [19].

The main components of a hip implant are the femur head and the acetabular cup (Figure 2A), which typically consists of either a ceramic or a polymeric liner housed in the so-called "metal back", which is fixed to the patient's pelvic bone [20,21]. While a "sandwich" design with a polymer layer between ceramic liner and acetabular cup has been tried, research on it has been discouraged by lower than average survival rates [22]. An all-ceramic acetabular cup, on the other hand, allows for a simpler monoblock design [23]. The prosthetic femur head is inserted into the femur bone after removal of the surgically resected original head: the femur stem holds a ball on top of it which is part of the ball and socket coupling that constitutes the prosthetic hip joint. The acetabular cup is the socket, and it is inserted in the pelvic bone. Joining the cup to the bone can be accomplished in many ways: however, the modern design of hip prostheses favours cementless acetabular cups, with a porous outer surface optimized for osseointegration [23]. The main issues are bone resorption, especially near the acetabular cup (Figure 2B,C), and loosening of the mechanical joint. High biocompatibility and cytocompatibility are needed to avoid bone resorption: this is regulated by wear particle release and the nature of debris, as well as the chemistry of materials and the stability and surface morphology of the implant. On the other hand, certain mechanical properties are also needed in order to obtain the longest possible lifespan and minimum particle release. In this regard, high wear resistance is very important, as is hardness, a low wear rate, good flexural strength and high fracture toughness. These properties are all exhibited by ceramic materials that are also very stable from a chemical viewpoint. However, not all ceramics exhibit the same performance.

For example, instability in the structure of zirconia under high stress and high humidity (tetragonal to monoclinic phase transformation) makes its fate unpredictable for long-term applications [24]. This is the reason why pure zirconia implants were withdrawn from the market and replaced by stabilized zirconia or alumina/zirconia composites (tradenamed as "Biolox delta") [25]. Alumina is still commercially available (tradenamed as "Biolox forte"), but its fracture toughness has proven insufficient under certain circumstances with the remote possibility of catastrophic failure, thus discouraging doctors from more widespread adoption and favouring "Biolox delta" instead. A recent study also highlighted that fracture in modern ceramic liners ("Biolox forte" and "Biolox delta") is mainly due to surgical errors/malpositioning rather than to inherent defects of the materials, which should virtually be nonexistent in certified commercial products [26].
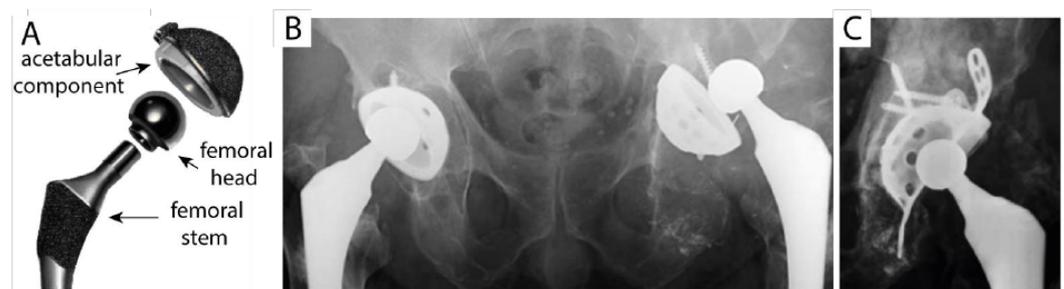

Figure 2. (**A**) Main components of a hip prosthesis, (**B**) displacement of the acetabular cup due to bone resorption, (**C**) same implant as picture (**B**) but shown at the moment of installation [1].

4. Silicon Carbide

4.1. Major Properties and Production Methods

Silicon carbide (SiC) is an advanced ceramic material discovered in the late 19th century by American inventor Edward G. Acheson, who was attempting to produce synthetic diamonds. Silicon carbide exhibits very interesting mechanical (see Table 2), electrical and electronic properties [27]. It possesses a wide band gap that makes it highly sought after for microelectronics and power electronics applications; good tensile strength even at high temperatures; decent fracture toughness under both static and dynamic conditions, which made it a popular choice for armour protection; good wear resistance; and high hardness, making it a recurrent choice in industrial tooling and abrasive application soon after its discovery. SiC is a polymorphic material and more than 250 polytypes have been found. While the planar disposition of atoms remains the same, the way different plans stack together can create a number of different microstructures, with the most researched being α-SiC and β-SiC. While a number of α structures have been designated, only one β structure exists, with a cubic layout often referred to as 3C-SiC. While monocrystalline SiC is the most relevant to electronics, polycrystalline and amorphous SiC are also studied for their mechanical properties [28].

Rarity in nature and high demand for many high-tech applications make for difficult procurement of raw materials, with price and availability often discouraging implementation. SiC is typically synthesized via the Acheson process, which was introduced in 1893. A mixture of silica and coal is heated in a furnace up to temperatures as high as 2480 °C and then gradually lowered. A few subreactions yield a combination of SiO_2 and coke to create SiC and carbon monoxide [29].The Acheson process does not really give much control over crystal growth and impurities. Thus, in 1955, the Lely growth method was introduced, which allowed for higher quality and higher purities, making way for further improvements and applications in electronics. The Acheson process still remains, at the moment, the most widespread way to produce silicon carbide for industrial applications, while evolutions of the Lely method dominate the electronics sector, where high purity, single crystals and precise crystal structures are needed. Other more "sustainable" but less common approaches for SiC production rely on the recycling of silicon slurry from

the semiconductor industry [30,31] or rice husk from the agricultural sector [32]. Silicon carbide is a brittle material for which machining is problematic and, like other ceramics, it is usually made into the final product via sintering or hot pressing for most industrial applications [27].

4.2. Biomedical Applications

Silicon carbide has also proven to be a highly biocompatible material, thus making it—together with its attractive physico-mechanical properties—very appealing in many biomedical applications. SiC has been studied for use in bone implants, hip implants, dental implants and cardiovascular stents, both as a structural component and as an adherent coating to reduce the release of potentially toxic metal ions. SiC composites also show interesting properties and will be discussed.

4.2.1. Porous Silicon Carbide for Bone Implant Applications

In the context of bone-contact applications, a special mention should be addressed to wood-derived porous SiC. Wood is a natural composite material, made up of a cellulose–hemicellulose matrix and a lignin-strengthening phase mixed within it [33]. The microstructure of wood looks similar to that of human bone tissue, and this inspired research for biomorphic silicon carbide, a porous material that manages to keep the microstructure of wood but swaps out wood itself for silicon carbide. This is accomplished via the silicon infiltration method: wood must be first dried and then pyrolyzed in argon in order to set up the carbon matrix, and after these early stages, silicon is infiltrated with or without any pressure applied. Properties of the end product depend on the porosity, which in turn is strictly dictated by the type of wood used [34] (as shown in Figures 3 and 4).
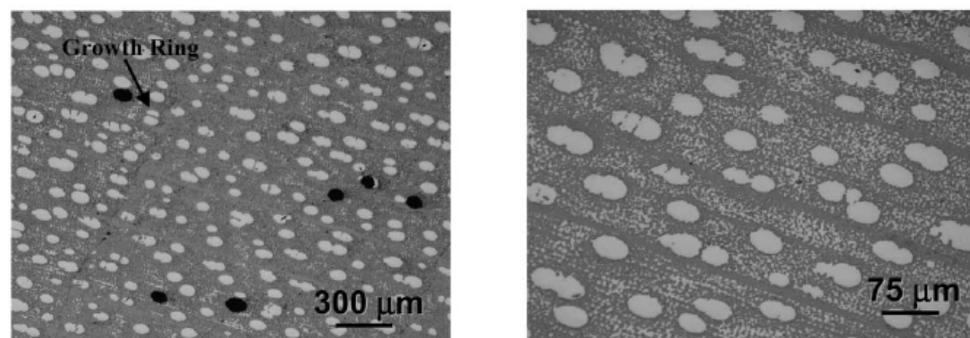

Figure 3. Optical micrograph of biomorphic Silicon Carbide made from maple wood (black = pores, white = Si, grey = SiC) [35].

Porosity directly affects the Young's modulus of a material; hence, increase porosity allows modulation to better simulate the elasticity of human bone tissue, with cortical bone having an average Young's modulus between 10 and 20 GPa and cancellous bone having an average Young's modulus in the range of 0.05 to 0.5 GPa [36]. This is important in order to reduce stress shielding, where the implant takes away stress from the living bone tissue, thus taking away the stimulus for the body to strengthen the latter, and eventually leading to weakening of the tissue in contact with the implant. Tensile and compression strengths, as well as fracture toughness, also diminish with increasing porosity.

Samples of SiC produced from mahogany and maple exhibit average flexural strengths (ASTM C 1161) of 144 and 344 MPa, average moduli of elasticity of 178 and 250 GPa and bulk densities of 2000 and 2270 kg/m^3 (ca 62% and 70% of theoretical density of SiC), respectively. The fracture toughness, as measured by the Chevron notch method (ASTM C 1421), which typically brings lower values as compared to other methods, is 2.6 MPa $\cdot$ m$^{\frac{1}{2}}$ for maple and 2 MPa $\cdot$ m$^{\frac{1}{2}}$ for mahogany [35]. These values, although far inferior to metals,

are similar to those of Al_2O_3, while their density is closer to human bone density, which is around 1900 kg/m^3 [37], compared to the 4500 kg/m^3 of titanium.
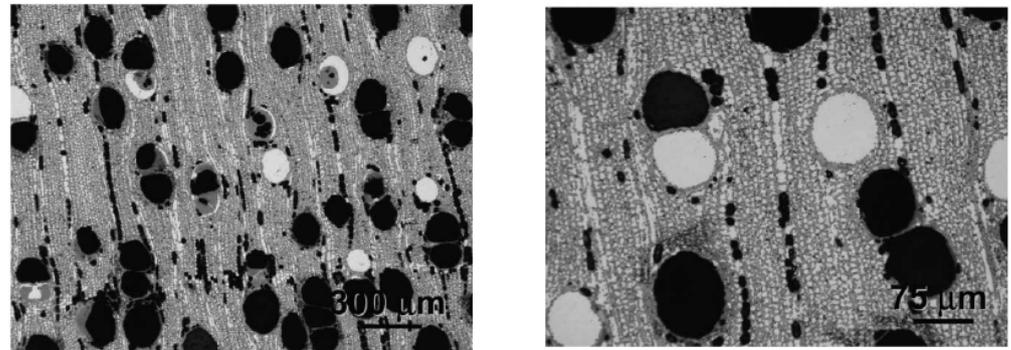

Figure 4. Optical micrographs of biomorphic silicon carbide made from mahogany wood (black = pores, white = Si, grey = SiC) [35].

Porous SiC can also be manufactured through more traditional and well-established sintering methods; in this case, however, a certain amount of sintering aid must be added to ceramic powders. Magnesium oxide has been researched for this application: specifically, a 3%wt. addition of MgO to SiC powder sintered at 1350 °C in open air resulted in a 24% porosity. Mechanical properties consist of a 80 GPa Young's modulus, a flexural strength of 180 MPa and a 3 MPa $\cdot$ m$^{\frac{1}{2}}$ fracture toughness, as measured by the Vickers indentation test [38]. However, in this particular case, it has been observed that the pores were too small to allow for vascularization; hence, more research is needed to improve this aspect, and the possibilities offered by wood-based SiC are becoming more interesting, both in terms of pore size and fabrication. Traditional sintering and hot pressing present limitations in the shape of the final product, because a mould is used. Biomorphic SiC, on the other hand, can be shaped before the wood is turned into SiC.

The biocompatibility of SiC is given not only by its chemical stability, abrasion resistance and low wear rates, but there is also evidence regarding the positive effects of Si ions on aspects such as bone growth [39,40]. Although the ion release of both vacuum sintered SiC and SiC-Mg has been measured to be higher in vitro compared with Ti$_6$Al$_4$V , it should be considered that with a porous material, the reacting surface of the ceramics was larger [38]. While SiC does cause immune response in vitro [41], it has been proven that it does not inhibit osteoblast and fibroblast activity, but it does not increase it either. In order to improve cell stimulation, silicon carbide can be coated with hydroxyapatite, a bioceramic known for its osteoconductive properties [42] (Figure 5).
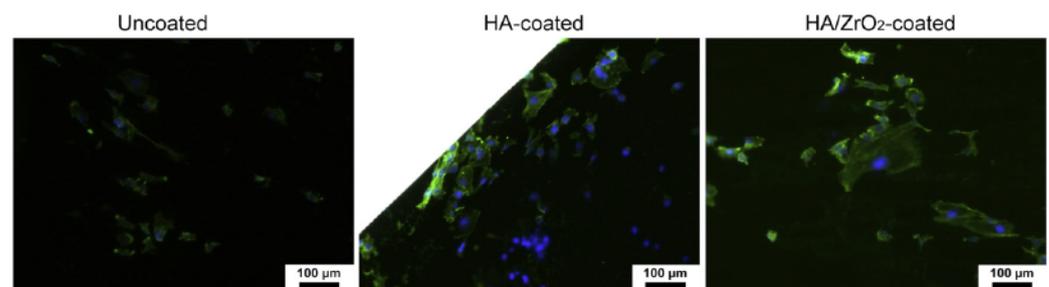

Figure 5. Fibroblasts highlighted in fluorescent images; cellular actin is in green and nuclei are in blue [42].

4.2.2. Silicon Carbide Thin Films

SiC can also be used to provide a biocompatible and protective coating to bone implant surfaces and bearing surfaces in particular to improve the life and safety of the device (Figure 6). This can be obtained mainly via chemical vapour deposition (CVD) and magnetron sputtering. Thin films are also used in the electronics field, and different crystal structures can be obtained with high precision, for example, by regulating the substrate temperature in the CVD process. However, amorphous silicon carbide (a-SiC) is the main crystal structure of interest for biomedical applications. Interestingly, this type of coating has already seen commercial clinical use through the German firm Biotronik Gmbh, used in cardiac stents under the trade name Rithron-XR™. Orthopedic applications might follow in the future. Microindentation on LPCVD SiC thin films shows a fracture toughness between 2.8 and 3.4 $MPa \cdot m^{\frac{1}{2}}$, with little dependence on crystal structure [43]. Thin films can be made in different thicknesses, the thinnest being made with Pulsed Laser Deposition (PLD), allowing for the production of SiC coatings free of defects with thicknesses of 30–100 nm and an average roughness of 1 nm [44]. Simulations made using molecular dynamics and Tersoff potential predict that the mechanical properties of 3C-SiC thin films above 10 nm in thickness converge with those of the bulk material [45]. At this scale, it has been observed that in response to relatively shallow indentation (105–208 nm), 3C-SiC goes through ductile deformation, changing its structure to a-SiC [46], which is an interesting property for tribological applications.
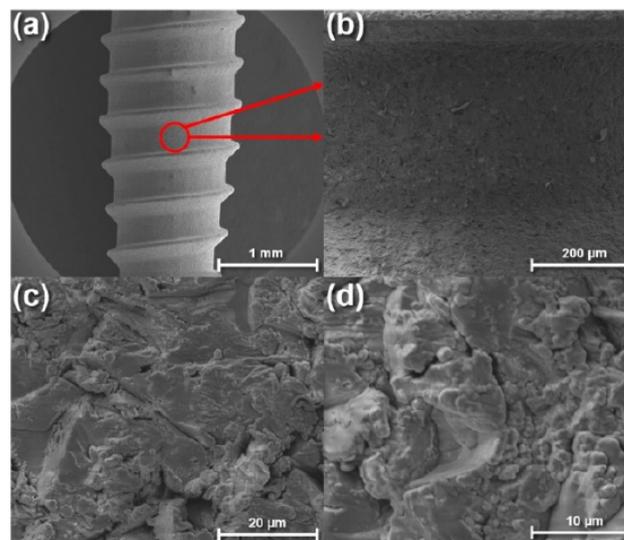

Figure 6. (**a**) Silicon carbide-coated titanium screw for biomedical applications, at different magnification to observe surface morphology (**b–d**) [27].

5. Silicon Nitride

5.1. Major Properties and Production Methods

Silicon nitride is an advanced ceramic material with properties that make it highly sought after in many different fields, from electronics to biomedical applications, gas turbines and sensors. Its strong covalent bonds give it high tensile and compressive strength, as well as hardness and wear resistance (see Table 2). Silicon nitride forms two hexagonal structures designed as α and β (Figure 7), and a third cubic one named γ which only occurs at high pressures and has no relevance for the topic reviewed. While covalent bonds dominate the long-distance order of Si_3N_4, an amorphous structure can be observed at the grain boundaries. The transformation of one structure to the other requires either solution–precipitation or an evaporation–condensation mass transport path. Therefore, even controlling the powder production process has a substantial impact on the final product's properties.
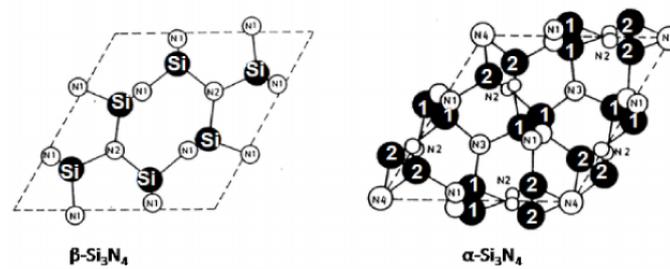
Figure 7. The α and β structures of silicon nitride [47].

Developed in 1859 by Deville and Wohler, Si_3N_4 did not gain widespread interest until the industrial process of reaction bonding was introduced commercially in the 1950s in the UK. Silicon powder was consolidated and nitrided between 1250 and 1300 °C: the result was a porous bulk silicon nitride or, via the same process, the Si_3N_4 "cake" could be milled to obtain a fine powder (around 85% Si_3N_4). Different cations tend to stabilize one structure or the other. Specifically, it has been found that iron (among other large cations), a common contaminant in commercial Si powders, promotes the growth of α-Si_3N_4, while β-Si_3N_4 is stabilized via the substitution of Si by Be or Al and O for N in solid solution phases. A large fraction (90%) of α structure is required to make strong SiN ceramics [48].

In the 1980s, Ube Industries introduced another type of silicon nitride powder, produced starting from $SiCl_4$ and NH_4 following the reaction:

$$SiCl_4 + NH_4 \longrightarrow Si(NH)_2 + NH_3Cl$$
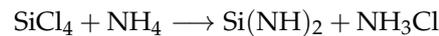
Silicon diimide is then pyrolized to Si_3N_4 at 1000 °C and heat-treated in nitrogen to produce α-Si_3N_4 (>95% of the powder). The major advantage is that $SiCl_4$ is a widely available, low-cost byproduct of silica ore processing [49].

Polycrystalline silicon nitride can easily achieve high fracture toughness values up to 11 MPa $\cdot$ m$^{\frac{1}{2}}$ (Table 2) due to a "beaver dam" microstructure, where single crystal whiskers are present, contrary to the equiaxial grain structure typical of most ceramic materials. Longer whiskers obstruct and deviate crack growth, allowing the material to tolerate more stress before reaching failure. Growth of this 'fibrous' microstructure can be facilitated by introducing β-Si_3N_4 whiskers in the silicon nitride powder before heat treatment. The powder must also contain over 75% α-Si_3N_4 [50].

Silicon nitride produced via sintering has excellent mechanical properties; however, it is extremely difficult to be made into complex shapes. This is a limiting factor for biomedical applications, and the difficulty of machining ceramic materials adds to the problem. The additive manufacturing (AM) of ceramics is being researched to expand the scope of silicon nitride applications. Several AM processes have been developed for silicon nitride, some of the most relevant being robocasting, selective laser sintering (SLS), stereolithography and binder 3D jet printing [51]. The last three AM technologies are mostly used to process non-oxide ceramics outside of the biomedical sector and, therefore, are not discussed in the present review. The optical properties of silicon nitride make direct SLS difficult; however, adding cold isostatic pressing (CIP) to the manufacturing process has shown improved mechanical properties [52], and SLS was successfully implemented to fabricate a biomedical-grade silicon nitride coating over titanium in one study [53]. Other processes such as a stereolithography apparatus (SLA), direct light processing (DLP), laser-induced slip (LIS) and laminated object manufacturing (LOM) have been tested, notably with the addition of Al_2O_3 in SLA [54], SiAlON/SiO_2 in DLP [55,56], SiC in binder jet (BJ) [57] to create ceramic composites and binder in the case of LOM to glue together the layers. The problem with these and other AM technologies is that while mechanical properties and the eventual presence of defects have been evaluated, biocompatibility has not. Although some of these processes have the potential to be used, in the future, to fabricate biomedical-grade components, more research with regards to biological properties is required.

5.2. Biomedical Applications

5.2.1. Robocasting of Silicon Nitride and Bone Scaffold Applications

Robocasting of Si_3N_4 has been researched for application in the biomedical field, with a focus on bone scaffold applications in which precise shaping and porosity are important requirements. Robocasting can be considered a variant of direct ink writing (DIW), with relatively higher solid loading ceramic ink.

It starts from a ceramic slurry, gel, paste or slip, which is extruded through a nozzle forming individual layers [58]. As a result, the final product is built up layerwise. Many studies have pointed out that high-density, defect-free components could be produced in this way while allowing for complex shapes. Sainz et al. [59] managed to produce highly porous Si_3N_4 structures for bone scaffold applications via a slurry printing process, using different sintering aids (alumina, silica and yttrium oxide) and a fraction of polymeric additive to give the necessary pseudoplastic behaviour. Printed structures were then sintered in a N_2 atmosphere or via spark plasma sintering. A value of 95% compared to theoretical density was reached, and shrinkage between 18 and 24% was registered; however, the latter might be predicted and compensated for during CAD design. Scaffolds had a flexural strength of 89 MPa and sufficient bioactivity. Alternatively, starting from an aqueous silicon nitride paste and forming different shapes with robocasting, followed by densification via sintering or hot isostatic pressing, has been shown to be suitable for producing an almost fully dense Si_3N_4 phase with a fibrous microstructure. Four-point bending tests showed a flexural strength of 552 MPa on average [60]. The dispersion of ceramic powders was improved by the addition of a cationic dispersant, as alumina and yttrium oxide sintering aids have negative charges on their surfaces. High- and low-molecular weight polyethylimine (PEI) was added to improve solid loading and viscosity during printing. Hydroxypropylmethyl cellulose (HPMC) was added as a viscosifying agent to make the slurry stronger. The biocompatibility of Si_3N_4 produced by robocasting has also been assessed [59]. Decreased concentrations of calcium and phosphate ions have been observed concurrently to the precipitation of hydroxyapatite upon immersion in simulated body fluids (SBF). Adsorption of albumin has been observed to happen almost instantly (less than 5 s) and the formation of a bovine serum albumin (BSA) molecule layer took around 300 s.

These properties are very valuable in bone scaffold applications, where compressive strength, as well as high porosity and biocompatibility, are needed. Scaffolds are used to aid bone tissue growth [61], such as in the case of spinal disc implants, often used to fuse together vertebrae in operations such as anterior cervical discectomy. A study compared PEEK, which has seen wide application and set the standard, with silicon nitride implants, both filled with autografts. Patients treated with silicon nitride and PEEK showed equal recovery, and no significant differences in clinical outcome have been observed up to 24 months. Spinal spacers are currently manufactured by CTL Amedica and available commercially under the trademark name Valeo C+CsC™. The fabrication process is not available to the public, but the manufacturer describes it as a composite made up of a porous core for osseoconduction and a dense outer part with structural capabilities (Figure 8).
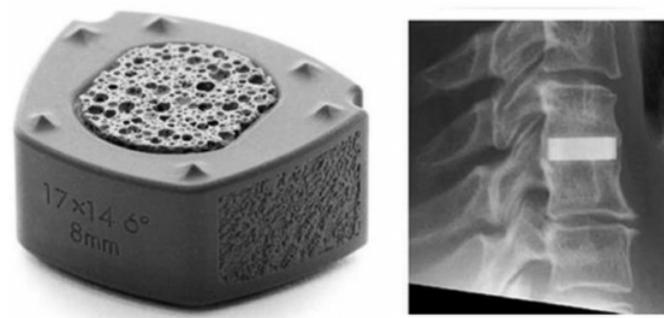

Figure 8. Valeo C+CsC™silicon nitride spinal implant manufactured by CTL Amedica [47].

5.2.2. Silicon Nitride for Biomedical Bearing Applications

Silicon nitride has seen use as a material for bearings, especially in harsh conditions such as rings and rolling surfaces at temperatures up to 1000 °C. It therefore appears logical that it could work as a bearing surface in bone implants such as hip prostheses, an apparently less demanding task. Studies have also been carried out to evaluate its use in less invasive implants such as hip resurfacing, where the femur head is not cut and replaced, but, as the name suggests, it only becomes resurfaced. Stress distributions in Si_3N_4-coated femurs have been found to replicate those of healthy bone well [62]. Silicon nitride, and particularly Al_2O_3-Y_2O_3 and in situ-toughened Si_3N_4, has been shown to have great stability in an environment similar to that of the human body, as found by testing after samples that have been kept in an autoclave (a common simulation for in vivo testing) for 100 h without any observable phase changes and unaltered flexural strength [63]. Friction coefficients measured for silicon nitride–silicon nitride couplings range widely from values as low as 0.002 to others as high as 0.8 [64]. This can be explained by the nature of wear mechanisms in silicon nitride, which is not only a mechanical wear process, such as what is seen in oxide ceramics, but also a tribochemical wear process. In this regard, the following reactions have been observed [65]:

$$Si_3N_4 + 6H_2O \longrightarrow 3SiO_2 + 4NH_3$$
$$SiO_2 + H_2O \longrightarrow Si(OH)_4$$
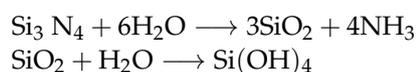
According to research, the tribochemical process is dominant at lower loads, higher speeds and during continuous motion. Low friction is measured in these conditions, caused by the smooth surfaces and a colloidal boundary film between components. Vice versa, the mechanical wear process is dominant at high loads, low speeds and stop–start motion, causing more friction between parts. It has been concluded that there is a minimum sliding velocity and a minimum dwell time that allow for tribochemical polishing, thus defining the interval of operation where minimal friction is measured [66].

Biocompatibility has been evaluated both in vitro and in vivo with successful results. L929 mice fibroblasts in contact with silicon nitride have been documented to have cell growth, viability and morphology comparable to those of titanium [67]. Even industrial-grade silicon nitride has shown favourable biocompatibility using the same L929 cell cultures compared with currently used titanium and alumina [68]. In vitro experiments claim good cytocompatibility using human osteoblast-like MG63 cells [69]. The in vivo behaviour of silicon nitride has also been assessed, using ad hoc hip prostheses implanted in pigs [70]. It was observed that 4 weeks after implantation, the tissues were engaging closely with the bone tissue, and 26 weeks after implantation, healthy, newly formed bone could be observed. Furthermore, CT scans confirmed healthy positioning and no foreign body reaction. It should be observed that adverse reactions with hip implants are usually detected over the course of a much longer period; however, it is reasonable that animal testing cannot be carried on for 20 or 30 years, which may be the timescale of prosthesis implanted in humans.

6. Diamond-like Carbon

6.1. Major Properties and Production Methods

Diamond-like carbon comprises a vast class of amorphous carbon materials, some containing over 50 at.% hydrogen (a-C:H) while others only contain as little as 1% hydrogen (a-C). DLC films are characterized by sp^3-type C bonds that give these materials physical and mechanical properties similar to those of diamond. The a-C:H films are usually made up of a less than 50% sp^3-hybridized carbon fraction, while a-C films typically contain 85% or more sp^3 bonds. The term "DLC" is more specifically used in reference to the hydrogenated form of diamond-like carbon (a-C:H). Non-hydrogenated carbon (a-C), on the other hand, is referred to as "taC" (tetrahedral carbon). DLC and taC are thermodynamically metastable materials and have to be prepared under ion bombardment of the growing films [71]. These films were first introduced in 1971 by Aisenberg and Chabot [72].

Currently, DLC can be deemed mature technology, while taC and its applications are still being explored and researched. Both these materials are produced by means of plasma-enhanced chemical vapour deposition (PECVD) or physical vapour deposition (magnetron sputtering or ion beams); however, other processes such as plasma source ion implantation (PSII) are also available. DLC coatings have already been used in industrial tools and in the famous Gillette MACH3 shaving product [73].

The production process of DLC has to occur in hydrogen-rich environments with a fraction of hydrogen between 10 and 50%. The substrate bias (i.e., electrical potential) controls the deposition rate and the structure of the material, and a negative bias is required as the grounded substrate has been shown to produce polymers. The superhard properties of taC films are achieved by the high energy of the particles forming the film. It is assumed that taC films grow by subplantation, while DLC usually grows by condensation.

The properties of DLC and taC are owed to their sp^3- and sp^2-hybridized bonds and their respective fractions (Figure 9). Angus and Jansen [74] have formulated a model to describe the structure of hydrogenated DLC, describing it as a covalent, fully constrained network model. According to their model, DLC's structure may be represented as a 3D array of mostly six-numbered rings, able to contain a fraction of the bound hydrogen in the range of 17–61 at.%. Hydrogen contributes to the carbon's diamond-like properties as it passivates dangling bonds in the amorphous structure and determines the film structure itself. Robertson [75] modelled the broader structure of DLC as a random network of covalently bonded atoms with a substantial medium range order at the nanometre scale. Other elements may be added in small concentrations to improve DLC's properties, with most modifications being performed in order to relieve the compressive stresses (via the incorporation of N, Si or metals) or to reduce surface energy and lower friction coefficient (F or Si-O incorporation).

DLC films can offer high hardness and high elastic modulus, but they also suffer from high internal stresses. The fraction of sp^3 C determines these mechanical properties, as well as the hybridization type that characterizes diamond. The hardness of DLC can range between 10 and 30 GPa, with a corresponding Young's modulus 6–10 times higher. However, the film structure is tensed up by an internal compressive stress of 0.5–7 GPa. Stresses may be reduced with the addition of N, Si, O or metals, but this is also detrimental to hardness and elastic modulus. The hardness and Young's modulus of taC films are markedly higher at 40–80 GPa and up to 900 GPa, respectively. However, higher internal stresses follow, measuring values of up to 13 GPa. To lower internal stresses, metals can be added or a high hardness layer can be combined with softer ones to create a multilavered structure.
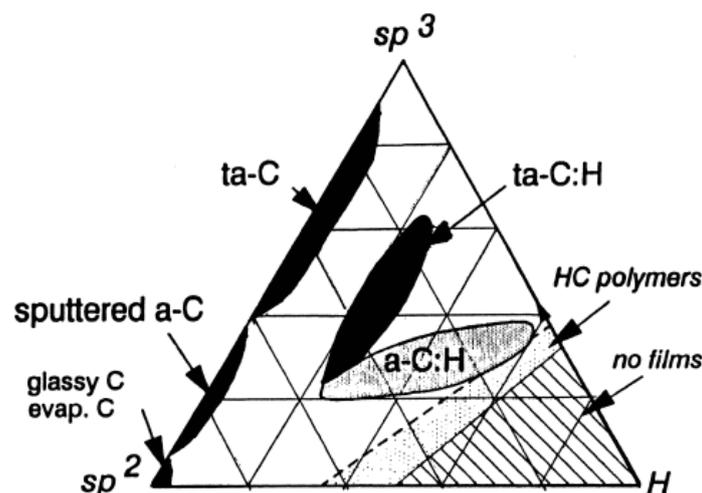

Figure 9. Schematization of carbon materials based on sp^3, sp^2 and hydrogen fractions [71].

Wear in DLC coatings occurs in the form of both abrasive wear and polishing wear, and researchers divide the process in four stages [76] (Figure 10). At first, asperities from the coating penetrate into the other contact surface because of pressure, and plastic flow of material around the coating occurs. In the second stage, the plugging of the counter surface causes abrasive wear, and an increase in carbon diffusion weakens bonds in coating asperities. The third stage involves increasing carbon diffusion, which results in micro-cleavage and polishing wear. Therefore, friction coefficient and roughness decrease. In the last stage, the friction coefficient is stabilized, following a strengthening of the counter surface and an increased smoothness of the coated surface. This process can be observed to a different extent for taC, although the wear resistance is generally higher for taC, with the counter surface wear also being higher [77] (Figure 11). Wear and fatigue have been proven to cause rehybridization in DLC and taC; this undesirable process causes sp^3 C to turn into sp^2 bonds, with the consequent formation of graphite on the wear surface [78]. On the other hand, graphitization is greatly reduced in highly humid environments, such as the human body [79].
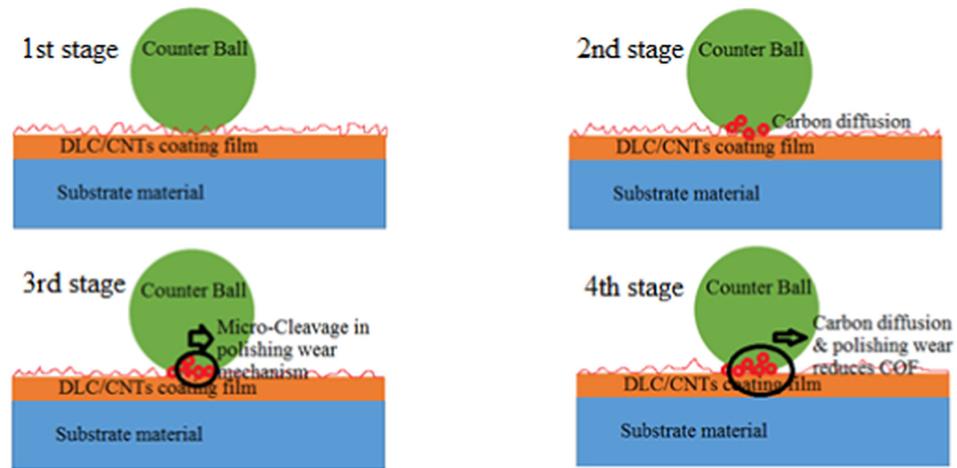

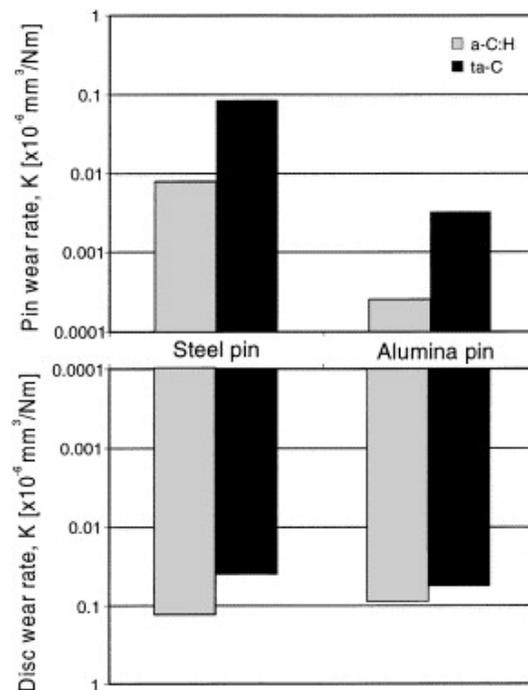**Figure 10.** Representation of the different stages of wear in DLC materials [76].

Figure 11. Wear rates of pin and disc in pin on disc friction test performed on a−C and a−C:H [77].

6.2. DLC for Biomedical Bearing Applications

DLC coatings have been successfully implemented to reduce friction in many applications; a popular example is its use in piston rings. Biomedical bearing applications require low friction and low wear rates to maximize the life of components and minimize adverse reactions in the body. DLC and taC coatings have been experimented with for a hip prosthesis application, where the femoral head was coated with DLC and taC. Microdimples were present on the contact surface as they have been successfully implemented in other applications to improve lubrication, specifically by creating a vortex in the microdimple, which improves hydrostatic pressure. Microdimples have been found to collect wear particles, thus slowing particle release, but also to reduce the overall hardness of the contact surface. The possible fluid movements that could transport wear particles out of the microdimples in this application are not yet fully documented. The results of the study show that both DLC and taC have a lower friction than stainless steel either with or without microdimples. While dimples very negligibly affected taC's friction coefficient (0.119 vs. 0.121), in DLC, microdimples resulted in a higher friction coefficient (0.107) than without the dimples (0.084), with a-C:H being the absolute lowest measured in terms of friction (Figure 12). The tribological properties were evaluated using a bovine serum solution at a temperature of 37 °C with a pendulum hip joint simulator to mimic a walking motion using a load of 1760 N, considered three times higher than the normal load on the joint [80].
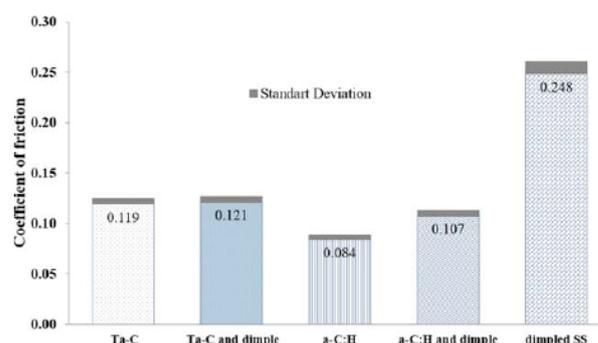

Figure 12. Friction coefficients of dimpled and non dimpled a−C, a−C:H and stainless steel [80].

The biocompatibility of DLC coatings on a porous titanium substrate has been evaluated in vivo using a DLC coating and nitrogen-containing carbon ($CN_{0.25}$). When considering the newly formed tissue after 4 weeks, samples with a coating showed a markedly stronger tissue in terms of relative (to native bone) bonding tensile strength. The same observation could be made after 16 weeks. While the relative bonding tensile strength at 52 weeks was equal for both coated and non-coated porous titanium, the DLC-coated titanium still had the highest fraction of mature neogenic tissue [81]. Moreover, another study found that DLC materials with a higher fraction of sp^3 are more biocompatible than those with a lower one. In both cases, however, a lower IL-6 cytokine response has been documented compared to a CoCrMo alloy, which was associated with an overall enhanced biocompatibility [82].

It has to be noted, however, that one clinical study with DLC-coated titanium femur heads has been carried out, showing a lower survival rate of implants after 8.5 years (55%) compared to Al_2O_3 when coupled with polyethylene. Surfaces of 19 retrieved DLC-coated heads showed signs of pitting on the diamond-carbon layers. SEM revealed the delamination of the carbon layer which caused excessive PE debris [83]. Therefore, new designs should be evaluated carefully; one major flaw that can be observed in this clinical application is the use of PE for the acetabular cup as DLC hardness and wear mechanisms might be better suited for harder metallic or ceramic materials.

7. Composites

Biomedical applications have a stringent set of requirements, and despite their outstanding properties, Si_3N_4 and SiC can be further optimized for this field in the form of composites. When these non-oxide ceramics are combined with other ceramics, the resulting composites can exhibit enhanced toughness or wear resistance. Polymer-infiltrated composites, on the other hand, can deliver very good mechanical properties with a lower elastic modulus to reduce stress shielding and improve implant longevity. DLC is mainly used for thin films; therefore, it will not be discussed in this section. However, its properties can be fine-tuned by way of doping, which has been mentioned in the previous section.

7.1. C/SiC Composites

Silicon carbide can be combined with other ceramics to create ceramic matrix composites, with improved properties for a number of applications. One interesting example is carbon fibre-reinforced SiC or C/SiC (Figure 13). Carbon fibres posses high tensile strength and a lower elastic modulus (compared with SiC) and also improve damage tolerance, making for an interesting combination for biomedical load-bearing applications. Moreover, the widespread use in the automotive sector has underlined the stable and low wear rate of the material. There are several C/SiC composites; however, not all of them are biocompatible and suitable for bone applications: this is primarily dependent on material composition [84]. One promising biomedical grade C/SiC composite has a fraction of 35% carbon fibre, 2–5% silicon, 55% SiC and 2–5% remaining carbon. Silicon and carbon are usually left after the silicon infiltration process used for production. Flexural strength has been detected to be 180 MPa with a Young's modulus between 120 and 150 GPa; in addition, the density has been measured to be between 2500 and 3000 kg/m^3. Another important detail is the low porosity around 1–3%. The friction coefficient, measured with a ceramic Al_2O_3 head, was reported to be 0.31 in dry conditions and 0.27 in calf serum. While these values are relatively high for tribological applications, they are compensated by wear resistance in ceramic on ceramic applications. It shall be noted that measurement was taken under higher pressure than usual at the contact interface [85].
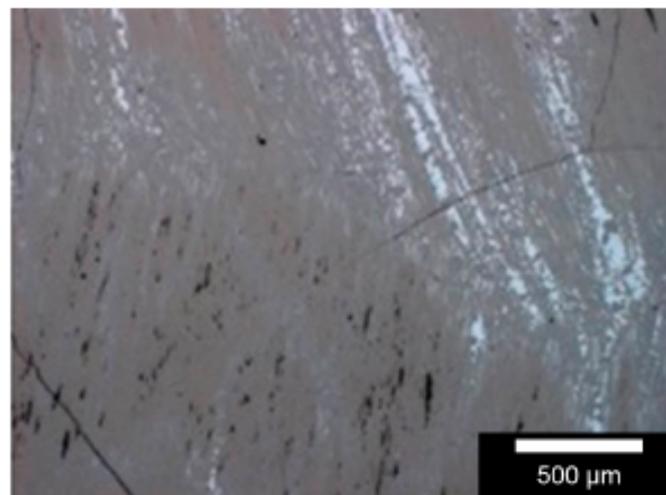

Figure 13. White light interferometric image of C/SiC; Pale grey = silicon; Dark grey = silicon carbide; Black = carbon fibres or pores [85].

In vitro biocompatibility test revealed the good viability of bone cells cultured on the material surface. Specifically, MG63 cells and primary osteoblasts were monitored for 21 days, and no morphologic aberrations were observed, while good adhesion and an increased number of cells per unit of surface area was found [85] (Figure 14).
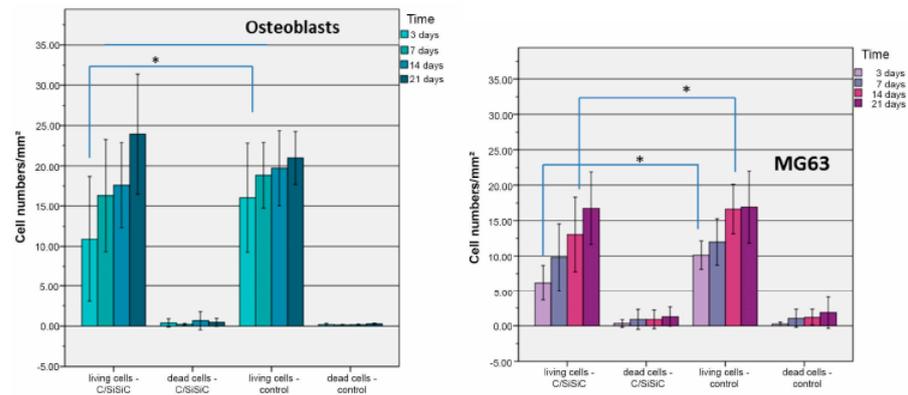
Figure 14. Cytotoxicity of C/SiC composite in terms of live and dead cells after 3, 7, 14 and 21 days of culture, * $p < 0.05$ [85].

7.2. Polymer-Infiltrated Silicon Nitride Composites

The main issue with silicon nitride bone implants is the high elastic modulus, which is one order of magnitude higher than that of human bone, thereby raising concerns for stress shielding. Porous materials have a lower Young's modulus, which is nonetheless still too high. An alternative route might be to create composites with low elastic modulus materials such as polymers, assuming that the component does not work as a bearing surface and the polymer material does not release too many wear particles. Such an experiment on polymer-infiltrated silicon nitride composites (PISNC) has been carried out for dental applications [86]. Silicon nitride was produced by gelcasting, coated with bonding agents and eventually infiltrated with polymethylmethacrylate (PMMA) (Figure 15), which was later cured in situ.
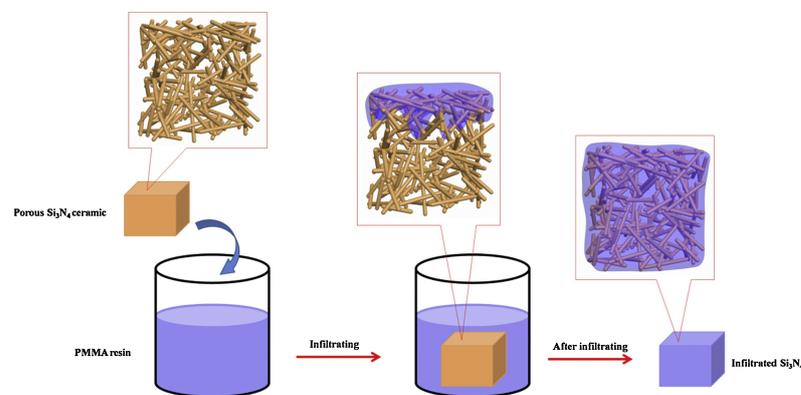

Figure 15. Process of silicon nitride matrix infiltration [86].

Ceramic solid contents of 50, 55 and 60 wt.%(PSN50, PSN55, PSN60) were tested and performed consistently better than the porous silicon nitride matrix alone. Higher solid content samples showed higher moduli of elasticity and flexural strengths, as could be expected (Figure 16), measuring an average of 56.1 GPa and 385.3 MPa, respectively. Lower average values of 52.1 GPa and 273 MPa were measured for the 50 wt.% samples, showing good balance between high flexural strength and a Young's modulus similar to that of cortical bone [87].

Biocompatibility was also examined with human gingival fibroblasts (HGF) and IL-6 cytokine release was assessed to evaluate cytocompatibility and inflammatory response. HGF cultures were observed at 1.4 and 24 h with an SEM microscope to evaluate adhesion to the surface compared to silicon nitride and PMMA. PSN60 showed a similar level of adhesion to Si_3N_4. Cell proliferation was evaluated with alamar blue fluorescence, showing a consistent increase in intensity and therefore number of live cells. Cytokine release levels

have been seen to be in line with medical PMMA (Figure 17). A similar approach (polymer infiltration) was also recently proposed to modulate the properties of alumina preforms for dental applications with promising results [88].
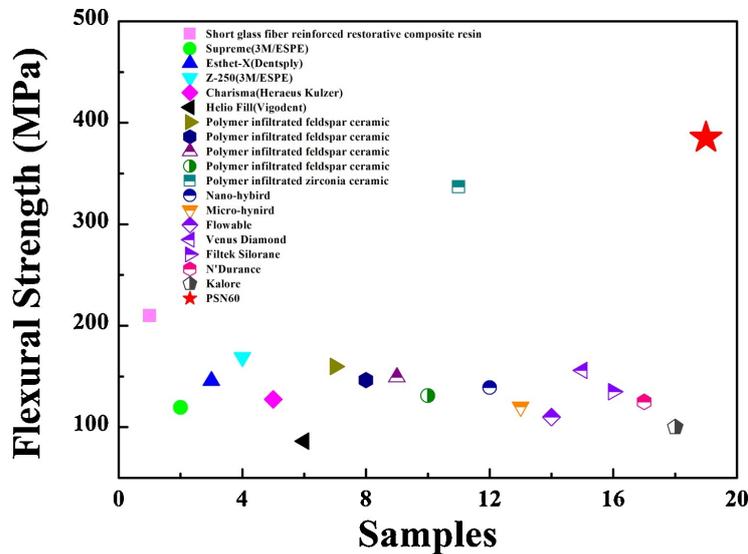

Figure 16. SN60 compared with other materials, silicon nitride and zirconia reinforced composites showing markedly superior flexural strength [86].
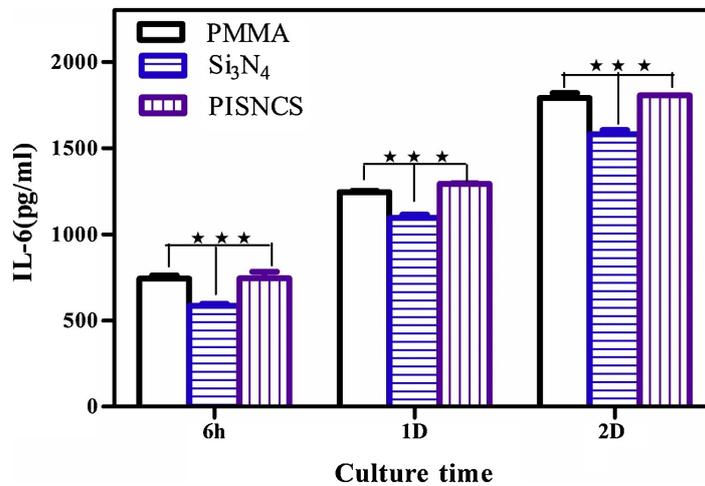

Figure 17. IL-6 cytokine response related to culture time on PMMA, silicon nitride and polymer-infiltrated silicon nitride composites, *** $p < 0.001$ [86].

7.3. Alumina-SiC

SiC was introduced as a reinforcing phase into matrices of alumina in an effort to obtain nanocomposites with superior mechanical properties as compared to the basic ceramic. As regards the former case, for example, the hardness and elastic modulus of $Al_2O_3/5$ vol% SiC nanocomposite were found to be 17.5 GPa and 405 GPa, respectively, which were slightly higher than the hardness (17 GPa) and elastic modulus (400 GPa) of pure alumina [89]. On the contrary, the results assessed for the fracture strength and fracture toughness of Al_2O_3/SiC nanocomposites, although generally showing some benefits, are controversial. In a study performed by Niihara and Nakahira [90], the fracture strength and fracture toughness of an $Al_2O_3/5$ vol% SiC nanocomposite were reported to be 1 GPa and 4.7 MPa $\cdot$ m$^{\frac{1}{2}}$, respectively, which revealed a significant improvement compared to the values of 400 MPa and 3 MPa $\cdot$ m$^{\frac{1}{2}}$ of pure alumina. However, other researchers have reported a significantly lower increment in fracture toughness (up to 20%) along with more

important increases in the fracture strength (up to 80%) for the same nanocomposites [91]. Perhaps the most interesting advantage of incorporating SiC nanoparticles into an alumina matrix is the increase in wear resistance, which is indeed a key added value for load-bearing applications of medical prostheses. In this regard, it has been clearly shown that the abrasion rate of Al_2O_3 can be greatly reduced through the addition of SiC nano-inclusions. In a wide set of wet erosion experiments where an aqueous slurry of Al_2O_3 particles was used, the wear rate of Al_2O_3/SiC nanocomposites was found to be half that of pure Al_2O_3 with an analogous grain size [92–95]. Rodriguez et al. [96] also reported that, under dry sliding conditions, the wear rate of pure Al_2O_3 was significantly higher (from three to five times) than that of Al_2O_3/SiC nanocomposites with analogous Al_2O_3 grain size (2–3 µm). The same study also highlighted the role played by grain size: in fact, the wear rate of an Al_2O_3/5 vol% SiC nanocomposite comprising an Al_2O_3 matrix with 0.7 µm grain size and SiC inclusions with 40 nm diameters was independent of the contact load and was 100 times lower than that of pure Al_2O_3.

7.4. SiC/Si₃N₄

As regards the potential reinforcement of a Si_3N_4 matrix with SiC nanoparticles, the data reported in the literature are controversial. In one study, Greskovich and Palm [97] observed that the fracture toughness and microhardness of Si_3N_4/SiC nanocomposites were not affected by the volume fraction of the secondary phase (SiC nanoparticles), which apparently yielded no beneficial effects. On the contrary, other papers from Niihara's research team [98–100] reported opposite conclusions, claiming that the strength and fracture toughness of Si_3N_4 can be significantly increased by the presence of SiC nano-inclusions. Perhaps these discrepancies are due to the different fabrication methods used to produce the composites, leading to different micro-/nano-structural characteristics which ultimately make the comparison among the studies difficult and even inconsistent.

8. Discussion and Conclusions

At present, biomedical applications of non-oxide ceramics show great promise in prosthetics and, more specifically, in the fabrication of acetabular cups for hip joint replacements. Clinical and societal challenges in this context are impressive. Safer alternatives to Al_2O_3, which has been documented to have a survival rate above 95% [101], might be found in non-oxide ceramics such as silicon carbide, silicon nitride and DLC. The most researched of the three for hip implants in particular are silicon nitride and DLC. These materials offer great biocompatibility and convenient tribological and mechanical properties (a comparison of pros and cons is summarized in Table 3). Modern design of acetabular cups tackles the problem of fitting larger femur heads as they allow for a more natural range of motion, and this can be made possible using thinner acetabular cups. For thinner acetabular cups to be safe, osseointegration is a critical issue. While all of the three presented materials have proven to be biocompatible, DLC and silicon nitride yield better osseointegration per se, while silicon carbide typically requires hydroxyapatite coating. Hence, a silicon nitride acetabular cup could be manufactured with a porous side for improved osseointegration and smooth contact surface, and its manufacturing could consist of a premade pressed cup on top of which robocasting could add the porous part and the two could then undergo sintering for consolidation. Toughened silicon nitride has a fracture toughness about twice that of ZTA and thrice that of ordinary alumina, thus making catastrophic failure less likely. In general, silicon nitride materials exhibit better mechanical behaviour as compared to oxide-based ceramics, such as alumina, which would indeed represent a benefit, explicitly in terms of an improved safety factor. In addition to its high fracture strength, which is comparable or even superior to that of composite oxides (e.g., alumina/zirconia ceramics), the most appealing property of silicon nitride is its quite high fracture toughness as compared to other ceramics. Moreover, spinal implants made of silicon nitride have shown adequate osseointegration and experiments either simulating hip implants or conducted in vivo suggest low wear rates (Figure 18), low friction thanks to the peculiar wear

mechanisms of silicon nitride and a lack of negative impacts from wear particles. There is already commercial interest in the development of silicon nitride hip and knee implants, with acetabular cup designs already being patented [102]. Silicon carbide, on the other hand, has drawn less interest because of its cost and fracture toughness comparable to alumina. On the other hand, silicon carbide can be significantly toughened [103], yielding a slightly inferior fracture toughness to silicon nitride, but still superior to alumina, and it can make for a smoother bearing surface in serum-like environments, without the transition to tribochemical wear found in silicon nitride [104]. C/SiC composites could also potentially make for an interesting biocompatible surface with low and constant wear rates. Additive manufacturing of a porous side on top of a compact one is also a possibility through powder bed selective laser sintering [105], but silicon carbide also requires a hydroxyapatite coating for proper osseointegration. DLC, while having impressive properties, has collected some controversial clinical evidence [106]. While all three materials need more research, the one closest to implementation is silicon nitride, with companies such as Amedica Corp. and SyntX Technologies already producing spinal implants made with this material. Silicon carbide might become an option, but at the moment, research on the topic is more oriented towards biosensors and advanced biomedical applications.
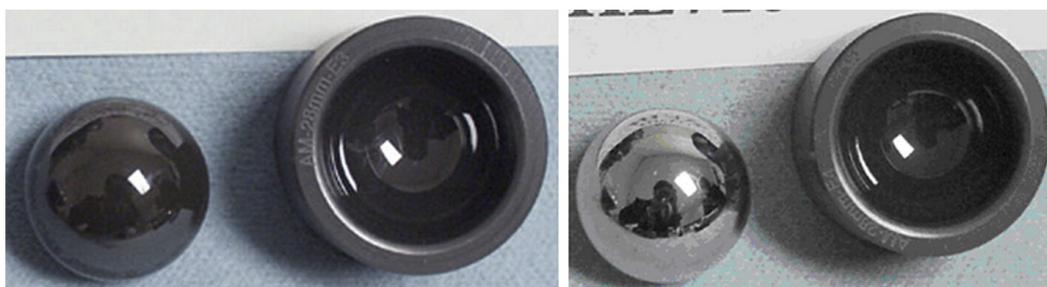

Figure 18. Silicon nitride acetabular cup and femur head before and after 1 million cycles [25] .

Table 3. Overview of the advantages and limitations of silicon nitride, silicon carbide and DLC .

Ceramic Type	Pros	Cons
Si_3N_4	Higher toughness than SiC, alumina, ZTA, DLC	Relatively higher friction coefficient compared with alumina, SiC
	Higher osteoconductivity than alumina, SiC, DLC	Relatively higher wear rate compared to SiC, alumina, DLC
SiC	Similar friction coefficient to alumina	Not osteoconductive, requires HA coating like alumina
	Can also be toughened to ZTA levels	More expensive than alumina, Si_3N_4
DLC	Lowest friction coefficient	Requires high hardness counter-surfaces, like alumina or Si_3N_4
	Lowest wear rate	Conflicting clinical evidence

Author Contributions: Conceptualization, C.M.P. and F.B.; Methodology, C.M.P. and F.B.; Writing— original draft preparation, C.M.P.; Writing—review and editing, F.B.; Supervision, F.B. All authors have read and agreed to the published version of the manuscript.

Institutional Review Board Statement: Not Applicable.

Informed Consent Statement: Not Applicable.

Data Availability Statement: Original data available in the cited references.

Conflicts of Interest: The authors declare no conflict of interest.

References

1. Ferrand, H.L.; Athanasiou, C.E. A materials perspective on the design of damage-resilient artificial bones and bone implants through additive/advanced manufacturing. *J. Miner. Met. Mater. Soc.* **2020**, *72*, 1195–1210. [CrossRef]
2. Deere, K.; Whitehouse, M.R.; Kunutsor, S.K.; Sayers, A.; Mason, J.; Blom, A.W. How long do revised and multiply revised hip replacements last? A retrospective observational study of the National Joint Registry. *Lancet Rheumatol.* **2022**, *4*, e468–e479. [CrossRef] [PubMed]
3. Duman, S.; Çamurcu, İ.Y.; Uçpunar, H.; Sevencan, A.; Akıncı, Ş.; Şahin, V. Comparison of clinical characteristics and 10-year survival rates of revision hip arthroplasties among revision time groups. *Arch. Med. Sci.* **2021**, *17*, 382–389. [CrossRef] [PubMed]
4. Bronzino, J.D.; Peterson, D.R. *The Biomedical Engineering Handbook*, 4th ed.; CRC Press: Boca Raton, FL, USA, 2015.
5. Eliaz, N. Corrosion of Metallic Biomaterials: A Review. *Materials* **2019**, *12*, 407. [CrossRef]
6. Kurtz, S.M. *The UHMWPE Handbook: Ultra-High Molecular Weight Polyethylene in Total Joint Replacement*; Elsevier Academic Press: San Diego, CL, USA, 2004.
7. Jackson, J. Father of the modern hip replacement: Professor Sir John Charnley (1911–1982). *J. Med. Biogr.* **2011**, *19*, 151–156. [CrossRef]
8. Sukur, E.; Akman, Y.E.; Ozturkmen, Y.; Kucukdurmaz, F. Particle Disease: A.Current Review of the Biological Mechanisms in Periprosthetic Osteolysis After Hip Arthroplasty. *Open Orthop. J.* **2016**, *10*, 241–251. [CrossRef]
9. Piconi, C. Oxide Ceramics for Biomedical Applications. In *Encyclopedia of Materials: Technical Ceramics and Glasses*; Elsevier: Amsterdam, The Netherlands, 2021; Volume 3, pp. 511–525.
10. Hannouche, D.; Zaoui, A.; Zadegan, F.; Sedel, L.; Nizard, R. Thirty years of experience with alumina-on-alumina bearings in total hip arthroplasty. *Int. Orthop.* **2011**, *35*, 207–213. [CrossRef]
11. Montazerian, M.; Hosseinzadeh, F.; Migneco, C.; Fook, M.V.L.; Baino, F. Bioceramic coatings on metallic implants: An overview. *Ceram. Int.* **2022**, *48*, 8987–9005. [CrossRef]
12. Jones, J.R.; Gentleman, E.; Polak, J. Bioactive glass scaffolds for bone regeneration. *Elements* **2007**, *3*, 393–399. [CrossRef]
13. Baino, F.; Fiume, E.; Barberi, J.; Kargozar, S.; Marchi, J.; Massera, J.; Verné, E. Processing methods for making porous bioactive glass-based scaffolds—A state-of-the-art review. *Int. J. Appl. Ceram. Technol.* **2019**, *16*, 1762–1796. [CrossRef]
14. Rezwan, K.; Chen, Q.Z.; Blaker, J.J.; Boccaccini, A.R. Biodegradable and bioactive porous polymer/inorganic composite scaffolds for bone tissue engineering. *Biomaterials* **2006**, *27*, 3413–3431. [CrossRef] [PubMed]
15. Bal, B.S.; Rahaman, M.N. Orthopedic applications of silicon nitride ceramics. *Acta Biomater.* **2012**, *8*, 2889–2898. [CrossRef] [PubMed]
16. Maximilien, E.; Launey, M.J.B.; Ritchie, R.O. On the mechanistic origins of toughness in bone. *Annu. Rev. Mater. Res.* **2010**, *40*, 25–53.
17. OECD. *Health at a Glance: OECD Indicators;* OECD Publishing: Paris, France, 2019.
18. Pezzotti, G.; Yamamoto, K. Artificial hip joints: The biomaterials challenge. *J. Mech. Behav. Biomed. Mater.* **2014**, *31*, 3–20. [CrossRef] [PubMed]
19. Knight, S.R.; Aujla, R.; Biswas, S.P. Total Hip Arthroplasty—Over 100 years of operative history. *Orthop. Rev.* **2011**, *3*, 2.
20. Latham, B.; Goswami, T. Effect of geometric parameters in the design of hip implants-paper IV. *Mater. Des.* **2006**, *25*, 287–307. [CrossRef]
21. Sargeant, A.; Goswami, T. Hip Implants: Paper V. Physiological Effects. *Mater. Des.* **2006**, *25*, 287–307. [CrossRef]
22. Kircher, J.; Bader, R.; Schroeder, B.; Mittelmeier, W. Extremely high fracture rate of a modular acetabular component with a sandwich polyethylene ceramic insertion for THA: A preliminary report. *Arch. Orthop. Trauma Surg.* **2009**, *129*, 1145–1150. [CrossRef]
23. Baino, F.; Minguella, J.; Kirk, N.; Montealegre, M.A.; Fiaschi, C.; Korkusuz, F.; Orlygsson, G.; Vitale-Brovarone, C. Novel full-ceramic monoblock acetabular cup with a bioactive trabecular coating: Design, fabrication and characterization. *Ceram. Int.* **2016**, *42*, 6833–6845. [CrossRef]
24. Clarke, I.C.; Manaka, M.; Green, D.D. Current status of zirconia used in total hip implants. *J. Bone Joint Surg. Am.* **2003**, *85*, 73–84. [CrossRef]
25. Rahman, M.N.; Yao, A.; Bal, B.S.; Garino, J.P.; Ries, N.D. Ceramics for prosthetic hip and knee joint replacement. *J. Am. Ceram. Soc.* **2007**, *90*, 1965–1988. [CrossRef]
26. Bistolfi, A.; Ferracini, R.; Lee, G.C.; Mellano, D.; Guidotti, C.; Baino, F.; Verné, E. Ceramic-on-ceramic catastrophic liner failure in total hip arthroplasty: Morphological and compositional analysis of fractured ceramic components. *Ceram. Int.* **2021**, *47*, 11029–11036. [CrossRef]
27. Saddow, S.E. Silicon Carbide Technology for Advanced Human Healthcare Applications. *Micromachines* **2022**, *13*, 346. [CrossRef] [PubMed]
28. Harris, G.L. *Properties of Silicon Carbide*; INSPEC: Manchester, UK, 1995; Volume 1, pp. 3–9.

29. Guichelaar, P.J. Acheson Process. In *Carbide, Nitride and Boride Materials Synthesis and Processing*; Chapman and Hall: London, UK, 1997; pp. 115–129.

30. Surek, T. Crystal growth and materials research in photovoltaics: Progress and challenges. *J. Cryst. Growth* **2005**, *275*, 292–304. [CrossRef]

31. Li, H.C.; Chen, W.-S. Recovery of silicon carbide from waste silicon slurry by using flotation. *Energy Procedia* **2017**, *136*, 53–59. [CrossRef]

32. Yalcin, N.; Sevinc, V. Studies on silica obtained from rice husk. *Ceram. Int.* **2001**, *27*, 219–224. [CrossRef]

33. Miller, R.B. *Wood Handbook—Wood as an Engineering Material*; USDA: Washington, DC, USA, 1999; Volume 2, pp. 2–6.

34. Greil, P.; Lifka, T.; Kaindl, A. Biomorphic Cellular Silicon Carbide Ceramics from Wood: II Mechanical Properties. *J. Eur. Ceram. Soc.* **1998**, *18*, 1975–1983. [CrossRef]

35. Singh, M.; Salem, J.A. Mechanical properties and microstructure of biomorphic silicon carbide ceramics fabricated from wood precursors. *J. Eur. Ceram. Soc.* **2002**, *22*, 2709–2717. [CrossRef]

36. Kaur, G.; Kumar, V.; Baino, F. Mechanical properties of bioactive glasses, ceramics, glass-ceramics and composites: State of the art review and future challenges. *Mater. Sci. Eng. C* **2019**, *104*, 109895. [CrossRef]

37. Cameron, J.R.; James, G.; Skofronick, R.M.G. *Physics of the Body*, 2nd ed.; Medical Physics Publishing: Madison, WI, USA, 1999; Volume 96.

38. Rade, K.; Martinčič, A.; Novak, S.; Kobe, S. Feasibility study of SiC-ceramics as a potential material for bone implants. *J. Mater. Sci.* **2013**, *48*, 5295–5301. [CrossRef]

39. Miguel, B.S.; Kriauciunas, R.; Tosatti, S.; Ehrbar, M.; Ghayor, C.; Textor, M.; Weber, F.E. Enhanced osteoblastic activity and bone regeneration using surface-modified porous bioactive glass scaffolds. *J. Biomed. Mater. Res. Part A* **2010**, *94*, 1023. [CrossRef] [PubMed]

40. Bal, B.S.; Rahaman, M.N.; Jayabalan, P.; Kuroki, K.; Cockrell, M.K.; Yao, J.Q.; Cook, J.L. In vivo outcomes of tissue-engineered osteochondral grafts. *J. Biomed. Mater. Res. Part B Appl. Biomater.* **2010**, *93*, 164–174.

41. Nordsletten, L.; Høgåsen, A.K.M.; Konttinen, Y.; Santavirta, S.; Aspenberg, P.; Aasen, A.O. Human monocytes stimulation by particles of hydroxyapatite, silicon carbide and diamond: In vitro studies of new prosthesis coatings. *Biomaterials* **1996**, *17*, 1521–1527. [CrossRef]

42. Gryshkov, O.; Klyui, N.I.; Temchenko, V.P.; Kyselov, V.S.; Chatterjee, A.; Belyaev, A.E.; Lauterboeck, L.; Iarmolenko, D.; Glasmacher, B. Porous biomorphic silicon carbide ceramics coated with hydroxyapatite as prospective materials for bone implants. *Mater. Sci. Eng.* **2016**, *68 C*, 143–152. [CrossRef]

43. Hatty, V.; Kahn, H. Fracture toughness of low-pressure chemical-vapor-deposited polycrystalline silicon carbide thin films. *J. Appl. Phys.* **2006**, *99*, 013517. [CrossRef]

44. Oujja, M.; Tabakkouht, K.; Sanz, M.; Rebollar, E.; Sánchez-Arenillas, M.; Marco, J.F.; Castillejo, M.; de Nalda, R. Synthesis of smooth amorphous thin films of silicon carbide with controlled properties through pulsed laser deposition. *Appl. Phys. A* **2022**, *128*, 375. [CrossRef]

45. Wang, W.-X.; Niu, L.-S.; Zhang, Y.-Y.; Lin, E.-Q. Tensile mechanical behaviors of cubic silicon carbide thin films. *Comput. Mater. Sci.* **2012**, *62*, 195–202. [CrossRef]

46. Zhao, L.; Zhang, J.; Pfetzing, J.; Alam, M.; Hartmaier, A. Depth-sensing ductile and brittle deformation in 3C-SiC under Berkovich nanoindentation. *Mater. Des.* **2021**, *197*, 109223. [CrossRef]

47. Heimann, R.B.; Nitride, S. A Close to Ideal Ceramic Material for Medical Application. *Ceramics* **2021**, *4*, 208–223. [CrossRef]

48. Riley, F.L. Silicon Nitride and Related Materials. *J. Am. Ceram. Soc.* **2000**, *83*, 245–265. [CrossRef]

49. Lange, F. The sophistication of ceramic science through silicon nitride studies. *J. Ceram. Soc. Jpn.* **2006**, *114*, 873–879. [CrossRef]

50. Lange, F.F. Relation Between Strength, Fracture Energy, and Microstructure of Hot-Pressed Si_3N_4. *J. Am. Ceram* **1973**, *56*, 518–522. [CrossRef]

51. Aguirre, T.G.; Cramer, C.L.; Mitchell, D.J. Review of additive manufacturing and densification techniques for the net- and near net-shaping of geometrically complex silicon nitride components. *J. Eur. Ceram. Soc.* **2022**, *42*, 735–743. [CrossRef]

52. Wang, K.J.; Bao, C.G.; Zhang, C.; Li, Y.; Liu, R.; Xu, H.; Song, S. Preparation of high-strength Si_3N_4 antenna window using selective laser sintering. *Ceram. Int.* **2021**, *47*, 28218–28225. [CrossRef]

53. Zanocco, M.; Boschetto, F.; Zhu, W.; Marin, E.; McEntire, B.J.; Bal, B.S.; Pezzotti, G. 3D-additive deposition of an antibacterial and osteogenic silicon nitride coating on orthopaedic titanium sub-strate. *J. Mech. Behav. Biomed.* **2020**, *103*, 103557. [CrossRef]

54. Xing, H.Y.; Zou, B.; Liu, X. Fabrication strategy of complicated Al_2O_3-Si_3N_4 functionally graded materials by stereolithography 3D printing. *J. Eur. Ceram. Soc.* **2020**, *40*, 5797–5809. [CrossRef]

55. Altun, A.A.; Prochaska, T.; Konegger, T.; Schwentenwein, M. Dense, strong, and precise silicon nitride-based ceramic parts by lithography-based ceramic manufacturing. *Appl. Sci.* **2020**, *10*, 996. [CrossRef]

56. Chen, R.F.; Duan, W.Y.; Wang, G.; Liu, B.; Zhao, Y.; Li, S. Preparation of broadband transparent Si_3N_4-SiO_2 ceramics by digital light processing (DLP) 3D printing technology. *J. Eur. Ceram. Soc.* **2021**, *41*, 5495–5504. [CrossRef]

57. Xiao, S.S.; Mei, H.; Han, D.; Yuan, W.; Cheng, L. Porous($SiCw$-Si_3N_4w)/(Si_3N_4-SiC) composite with enhanced mechanical performance fabricated by 3D printing. *Ceram. Int.* **2018**, *44*, 14122–14127. [CrossRef]

58. Peng, E.; Zhang, D.; Ding, J. Ceramic robocasting: Recent achievements, potential, and future developments. *Adv. Mater.* **2018**, *30*, 1802404. [CrossRef]

59. Sainz, M.A.; Serena, S.; Belmonte, M.; Miranzo, P.; Osendi, M.I. Protein adsorption and in vitro behavior of additively manufactured 3D-silicon nitride scaffolds intended for bone tissue engineering. *Mater. Sci. Eng. C* **2020**, *115*, 110734. [CrossRef]

60. Zhao, S.; Xiao, W.; Rahaman, M.N.; O'Brien, D.; Seitz-Sampson, J.W.; Bal, B.S. Robocasting of silicon nitride with controllable shape and architecture for biomedical applications. *Appl. Ceram. Technol.* **2017**, *14*, 117–127. [CrossRef]

61. Baino, F.; Novajra, G.; Vitale-Brovarone, C. Bioceramics and scaffolds, a winning combination for tissue engineering. *Front. Bioeng. Biotechnol.* **2015**, *3*, 202. [CrossRef] [PubMed]

62. Zhang, W.; Titze, M.; Cappi, B.; Wirtz, D.C.; Telle, R.; Fischer, H. Improved mechanical long-term reliability of hip resurfacing prostheses by using silicon nitride. *J. Mater. Sci. Mater. Med.* **2010**, *21*, 3049–3057. [CrossRef] [PubMed]

63. Bal, B.S.; Khandkar, A.; Lakshminarayanan, R.; Clarke, I.; Hoffman, A.A.; Rahaman, M.N. Testing of silicon nitride ceramic bearings for total hip arthroplasty. *J. Biomed. Mater. Res. B* **2008**, *87*, 447–454. [CrossRef] [PubMed]

64. Park, D.S.; Danyluk, S.; McNallan, M.J. Influence of tribochemical reaction products on friction and wear of silicon nitride at elevated temperatures in reactive environments. *J. Am. Ceram. Soc.* **1992**, *75*, 3033–3039. [CrossRef]

65. Tomizawa, H.; Fischer, T.E.; Trans, A. Friction and Wear of Silicon Nitride and Silicon Carbide in Water: Hydrodynamic Lubrication at Low Sliding Speed Obtained by Tribochemical Wear. *ASLE Trans.* **1988**, *30*, 41–46.

66. Zhou, Y.S.; Ohashi, M.; Tomita, N.; Ikeuchi, K.; Takashima, K. Study on the possibility of silicon nitride-silicon nitride as a material for hip prostheses. *Mater. Sci. Eng.* **1997**, *5 C*, 125–129. [CrossRef]

67. Neumann, A.; Jahnke, K.; Maier, H.R.; Ragoß, C. Biocompatibility of silicon nitride ceramic in vitro. A comparative fluorescence-microscopic and scanning. *Laryngorhinootologie* **2004**, *83*, 845–851. [CrossRef]

68. Neumann, A.; Reske, T.; Held, M.; Jahnke, K.; Ragoss, C.; Maier, H.R. Comparative investigation of the biocompatibility of various silicon nitride ceramic qualities in vitro. *J. Mater. Sci. Mater. Med.* **2004**, *15*, 1135–1140. [CrossRef]

69. Kue, R.; Sohrabi, A.; Nagle, D.; Frondoza, C.; Hungerford, D. Enhanced proliferation and osteocalcin production by human osteoblast-like MG63 cells on silicon nitride ceramic discs. *Biomaterials* **1999**, *20*, 1195–1201. [CrossRef]

70. Kong, X.; Hu, X.; Chai, W. In Vitro & In Vivo investigation of the silicon nitride ceramic hip implant's safety and effectiveness evaluation. *J. Orthop. Surg. Res.* **2022**, *17*, 87. [PubMed]

71. Grill, A. Diamond-like carbon: State of the art. *Diam. Relat. Mater.* **1999**, *8*, 428–434. [CrossRef]

72. Aisenberg, S.; Chabot, R. Ion-Beam Deposition of Thin Films of Diamondlike Carbon. *J. Appl. Phys.* **1971**, *42*, 2953–2958. [CrossRef]

73. Hahn, S.S.-H.; Madeira, J.; Chou, C.P.; Brooks, L.E. Razor Blade Technology. US Patent 5669144. 7 November 1995.

74. Angus, J.C.; Jansen, F. Dense "diamondlike" hydrocarbons as random covalent networks. *J. Vac. Sci. Technol.* **1988**, *6*, 1778–1782. [CrossRef]

75. Robertson, J.; O'Reilly, E.P. Electronic and atomic structure of amorphous carbon. *Phys Rev. B* **1987**, *35*, 2946–2957. [CrossRef]

76. Tyagi, A.; Walia, R.S.; Murtaza, Q.; Pandey, S.M.; Tyagi, P.K.; Bajaj, B. A critical review of diamond like carbon coating for wear resistance applications. *Int. J. Refract. Met. Hard Mater.* **2019**, *78*, 107–122. [CrossRef]

77. Ronkainen, H.; Varjus, S.; Koskinen, J.; Holmberg, K. Differentiating the tribological performance of hydrogenated and hydrogen-free DLC coatings. *Wear* **2001**, *249*, 260–266. [CrossRef]

78. Kunze, T.; Posselt, M.; Gemming, S.; Seifert, G.; Konicek, A.R.; Carpick, R.W.; Pastewka, L.; Moseler, M. Wear, Plasticity and Rehybridization in Tetrahedral Amorphous Carbon. *Tribol. Lett.* **2014**, *53*, 119–126. [CrossRef]

79. Liu, Y.; Erdemir, A.; Meletis, E.I. Influence of environmental parameters on the frictional behavior of DLC coatings. *Surf. Coat. Technol.* **1997**, *94–95*, 463–468. [CrossRef]

80. Choudhury, D.; Ching, H.A.; Mamat, A.B.; Cizek, J.; Osman, N.A.A.; Vrbka, M.; Hartl, M.; Krupka, I. Fabrication and characterization of DLC coated microdimples on hip prosthesis heads. *J. Biomed. Mater. Res. Part B* **2015**, *103*, 1002–1012. [CrossRef]

81. Rubstein, A.P.; Makarova, E.B.; Trakhtenberg, I.S.; Kudryavtseva, I.P.; Bliznets, D.G.; Philippov, Y.I.; Shlykov, I.L. Osseointegration of porous titanium modified by diamond-like carbon and carbon nitride. *Diam. Relat. Mater.* **2012**, *22*, 128–135. [CrossRef]

82. Liao, T.T. Biological responses of diamond-like carbon (DLC) films with different structures in biomedical application. *Mater. Sci. Eng.* **2016**, *C 69*, 751–759. [CrossRef]

83. Taeger, G.; Podleska, L.E.; Schmidt, B.; Ziegler, M.; Nast-Kolb, D. Comparison of diamond-like carbon and alumina oxide articulating with polyethylene in total hip anthroplasty. *Matwiss. Werkst.* **2003**, *34*, 1094–1100. [CrossRef]

84. Berndt, W.K.F. C/C–SiC composites for space applications and advanced friction systems. *Mater. Sci. Eng.* **2005**, *A 412*, 177–181.

85. Reichert, A.; Seidenstuecker, M.; Gadow, R.; Mayr, H.O.; Suedkamp, N.P.; Latorre, S.H.; Weichand, P.; Bernstein, A. Carbon-Fibre-Reinforced SiC Composite (C/SiSiC) as an Alternative Material for Endoprosthesis: Fabrication, Mechanical and In-Vitro Biological Properties. *Materials* **2018**, *11*, 316. [CrossRef] [PubMed]

86. Wang, F.; Guo, J.; Li, K.; Sun, J.; Zeng, Y.; Ning, C. High strength polymer/silicon nitride composites for dental restorations. *Dent. Mater.* **2019**, *35*, 1254–1263. [CrossRef] [PubMed]

87. Reilly, D.T.; Burstein, A.H.; Frankel, V.H. The elastic modulus for bone. *J. Biomech.* **1974**, *7*, 271–275. [CrossRef]

88. Crispim da Silveira, O.; Rodrigues, A.M.; Montazerian, M.; de Lucena Lira, H.; Baino, F.; Menezes, R.R. Al_2O_3 preforms infiltrated with polymethyl methacrilate for dental prosthesis manufacturing. *Appl. Sci.* **2021**, *11*, 7583. [CrossRef]

89. Niihara, K. New Design Concept of Structural Ceramics–Ceramic Nanocomposites. *J. Ceram. Soc. Jpn.* **1991**, *99*, 974–982. [CrossRef]

90. Niihara, K.; Nakahira, A. Strengthening and toughening mechanisms in nanocomposite ceramics. *Ann. Chim.* **1991**, *16*, 479–486.
91. Zhao, J.; Stearns, L.C.; Harmer, M.P.; Chan, H.M.; Miller, G.A.; Cook, R.F. Mechanical Behavior of Alumina–Silicon Carbide Nanocomposites. *J. Am. Ceram Soc.* **1993**, *76*, 503–510. [CrossRef]
92. Davidge, R.W.; Twigg, P.C.; Riley, F.L. Effects of Silicon Carbide Nano-phase on the Wet Erosive Wear of Polycrystalline Alumina. *J. Eur. Ceram. Soc.* **1996**, *16*, 799–802. [CrossRef]
93. Davidge, R.W.; Riley, F.L. Grain-Size Dependence of the Wear of Alumina. *Wear* **1995**, *45*, 186–187. [CrossRef]
94. O'Sullivan, D.; Hampshire, S.; Kennedy, T. Fabrication, Properties, and Modeling of Engineering Ceramics Reinforced with Nanoparticles of Silicon Carbide. *Br. Ceram. Trans.* **1996**, *96*, 121–127.
95. Sternitzke, M.; Dupas, E.; Twigg, P.; Derby, B. Surface Mechanical Properties of Alumina Matrix Nanocomposites. *Acta Mater.* **1997**, *45*, 3963–3973. [CrossRef]
96. Rodríguez, J.; Martín, A.; Pastor, J.Y.; Llorca, J.; Bartolomé, J.F.; Moya, J.S. Sliding Wear of Alumina/Silicon Carbide Nanocomposites. *J. Am.Ceram. Soc.* **1999**, *82*, 2252–2254. [CrossRef]
97. Greskovich, C.; Palm, J.A. Observations on the Fracture Toughness of b-Si$_3$N$_4$–b-SiC Composites. *J. Am. Ceram. Soc.* **1980**, *63*, 597–599. [CrossRef]
98. Sasaki, G.; Nakase, H.; Suganuma, K.; Fujita, T.; Niihara, K. Mechanical Properties and Microstructure of Si$_3$N$_4$ Matrix Composite with Nanometer Scale SiC Particles. *J. Ceram. Soc. Jpn.* **1992**, *100*, 536–540. [CrossRef]
99. Hirano, T.; Niihara, K. Microstructure and Mechanical Properties of Si$_3$N$_4$/SiC Composites. *Mater. Lett.* **1995**, *22*, 249–254. [CrossRef]
100. Sawaguchi, K.T.; Niihara, K. Mechanical and Electrical Properties of Silicon Nitride–Silicon Carbide Nanocomposite Material. *Mater. Lett.* **1991**, *74*, 1142–1144. [CrossRef]
101. El-Desouky, I.I. Ten-year survival of ceramic-on-ceramic total hip arthroplasty in patients younger than 60 years: A systematic review and meta-analysis. *J. Orthop. Surg. Res.* **2021**, *16*, 679. [CrossRef] [PubMed]
102. Ely, K.S.; Khandkar, A.C.; Lakshminarayanan, R.; Hofmann, A.A. Hip Prosthesis with Monoblock Ceramic Acetabular Cup. U.S. Patent No. 7695521, 13 April 2010.
103. Padture, N.P. In Situ-Toughened Silicon Carbide. *J. Am. Ceram. Soc.* **1994**, *77*, 519–523. [CrossRef]
104. Kusaka, J.; Takashima, K.; Yamane, D.; Ikeuchi, K. Fundamental study for all-ceramic artificial hip joint. *Wear* **1999**, *225–229*, 734–742. [CrossRef]
105. Grossin, D.; Montón, A.; Navarrete-Segado, P.; Özmen, E.; Urruth, G.; Maury, F.; Maury, D.; Frances, C.; Tourbin, M.; Lenormand, P.; et al. A review of additive manufacturing of ceramics by powder bed selective laser processing (sintering/melting): Calcium phosphate, silicon carbide, zirconia, alumina, and their composites. *Open Ceram.* **2021**, *5*, 100073. [CrossRef]
106. Love, C.A.; Cook, R.B.; Harvey, T.J.; Dearnley, P.A.; Wood, R.J.K. Diamond like carbon coatings for potential application in biological implants—A review. *Tribol. Int.* **2013**, *63*, 141–150. [CrossRef]